Cleaner Energy Systems 9 (2024) 100151

Contents lists available at ScienceDirect

Cleaner Energy Systems

journal homepage: www.elsevier.com/locate/cles

Battery remaining useful life estimation based on particle swarm optimization-neural network

Zuriani Mustaffa [a,*], Mohd Herwan Sulaiman [b]

[a] Faculty of Computing, Universiti Malaysia Pahang Al-Sultan Abdullah 26600 Pekan, Pahang, Malaysia
[b] Faculty of Electrical and Electronic Engineering Technology, Universiti Malaysia Pahang Al-Sultan Abdullah 26600 Pekan, Pahang, Malaysia

ARTICLE INFO

Keywords:
Battery Remaining Useful Life (RUL)
Lithium-ion batteries (LIBS)
Particle Swarm Optimization (PSO)
Neural Networks

ABSTRACT

Determining the Remaining Useful Life (RUL) of a battery is essential for several purposes, including proactive maintenance planning, optimizing resource allocation, preventing unforeseen failures, improving safety, extending battery lifespan, and achieving accurate cost savings. Concerning that matter, this study proposed hybrid Particle Swarm Optimization–Neural Network (PSO—NN) for estimating battery RUL. In the evaluation of the proposed method, the effectiveness is assessed using the metrics of Mean Absolute Error (MAE) and Root Mean Squared Error (RMSE). The dataset employed for this investigation comprises eight input parameters and one output variable, representing the battery RUL. In conducting an analysis, the performance of the PSO—NN model is compared with hybrid NN with Cultural Algorithm (CA-NN) and Harmony Search Algorithm (HSA-NN), as well as the standalone Autoregressive Integrated Moving Average (ARIMA). Upon examination of the findings, it becomes evident that the PSO—NN model outperforms the alternatives with an MAE of 2.7708 and an RMSE of 4.3468, significantly lower than HSA-NN (MAE: 22.0583, RMSE: 34.5154), CA-NN (MAE: 9.1189, RMSE: 22.4646), and ARIMA (MAE: 494.6275, RMSE: 584.3098). The PSO—NN also achieves the lowest maximum error of 104.7381 compared to 490.3125 for HSA-NN, 827.0163 for CA-NN, and 1,160.0000 for ARIMA. Additionally, the low two-tail probability values (P($T \leq t$)), all below the significance level of 0.05, indicate that the differences between PSO—NN and the other methods (HSA-NN, CA-NN, and ARIMA) are statistically significant. These results highlight the superior accuracy and robustness of the PSO—NN model in predicting battery RUL. This study contributes to the field by presenting the PSO—NN as a highly effective tool for accurate battery RUL estimation, as evidenced by its superior performance over alternative methods.

1. Introduction

The application of machine learning techniques, such as Support Vector Machines (SVM) (Vapnik, 1995), Neural Networks (NN), and Least Squares Support Vector Machines (LSSVM) (Suykens et al., 2002), to name a few, can be seen extensively and efficiently applied across diverse domains, including medical health (Abut et al., 2024; Mall et al., 2023), building engineering (Marzouk et al., 2024; Vivian et al., 2024), seismology (Gonzalez et al., 2022; Maya et al., 2022), smart agricultural (Mendoza-Bernal et al., 2024), ocean engineering (Hayati et al., 2024), finance (Gupta and Nalavade, 2023), automotive industry (Li et al., 2022; Li et al., 2024; Zhang et al., 2015) among others. Within the automotive sector, the growing adoption of electric vehicles has sparked significant research into Battery Management Systems (BMS) (Sulaiman and Mustaffa, 2024), as reducing fossil fuel consumption is crucial for promoting sustainable and healthy societal development (Zuo et al., 2022; Zuo et al., 2024). Leading automobile manufacturers worldwide have actively advanced the development of electric vehicles (Li et al., 2022), including both pure electric vehicles and hybrid electric vehicles (Zhang et al., 2022; Zuo et al., 2022), resulting in a significant increase in their presence on the roads. This growth has highlighted the critical role of Battery Management Systems (BMS) in ensuring the proper functioning of the battery, which is essential for the safety and efficiency of both the battery and vehicle operations. The BMS monitors and controls the battery pack's operational conditions, such as temperature, voltage, and current. It also conducts State of Charge (SoC) estimations to determine the remaining capacity of the battery and State of Health (SoH) assessments to measure the remaining lifespan of the battery (Mehta et al., 2024). Lithium-ion batteries (LIBs), serving as the core of new energy vehicles, have attracted increased attention. In recent years,

* Corresponding author.
E-mail address: zuriani@ump.edu.my (Z. Mustaffa).

https://doi.org/10.1016/j.cles.2024.100151
Received 16 May 2024; Received in revised form 14 September 2024; Accepted 27 September 2024
Available online 29 September 2024

as battery technology has advanced, batteries, functioning as the primary power source or energy storage component in devices, have witnessed widespread utilization (Zhou et al., 2023). Estimating the Remaining Useful Life (RUL), SoC, and SoH is crucial for effective proactive maintenance planning. It aids in optimizing resource allocation, preventing unexpected failures, improving safety measures, extending battery lifespan, and achieving accurate cost saving (Alsuwian et al., 2024). This is proven with numerous studies, particularly using machine learning techniques as presented in (Duan et al., 2023; Korkmaz, 2023; Li et al., 2022; Li et al., 2024; Rauf et al., 2022; Tao et al., 2024).

When working with ML techniques, such as NN and SVM, their effectiveness for estimation tasks is well-established. However, the performance of these models largely depends on optimizing key hyper-parameters. For instance, in the case of NN, hyper-parameters such as network weights and hidden layer biases require careful tuning, while in SVM, hyper-parameters such as the regularization parameter (C) and the kernel function need careful adjustment. Additionally, configuring elements like the appropriate number of hidden neurons for NN is crucial for achieving optimal results.

In response to that, a significant number of hybrid machine learning with optimization techniques have been demonstrated, aiming to automatically optimize the relevant hyper-parameters. Recently, the academic community has shown considerable interest in optimization using meta-heuristic algorithms, acknowledging their effectiveness in tackling current problems. Example of meta-heuristic algorithms are Moth Flame Algorithm (MFO) (Mirjalili, 2015), Salp Swarm Algorithm (SSA) (Mirjalili et al., 2017), Barnacles Mating Optimizer (BMO) (Sulaiman et al., 2020), Artificial Bee Colony (ABC), Bees Algorithm (BA), Genetic Algorithm (GA) (Haupt and Haupt, 2004), Differential Evolution, Grey Wolf Optimizer (GWO) (Mirjalili et al., 2014), Particle Swarm Optimization (PSO) (Kennedy and Eberhart, 1995) and many others.

Numerous hybrid machine learning with optimization algorithms have been demonstrated, such as study in (Dou et al., 2022) which introduced a hybrid methods combining the Salp Swarm Algorithm (SSA) with Extreme Learning Machine (ELM) for SoC estimation. To address the limitations of SSA in global search capability, the Sine Cosine Algorithm (SCA) was integrated into SSA. The study's findings suggest the superiority of SCA-SSA-ELM in comparison to SSA-ELM and a few other identified algorithms. In (Liu et al., 2022), a hybrid SVM with improved Barnacles Mating Optimizer was presented in estimating the SoC for LIBs. Another hybrid machine learning with BMO also can be seen in (Mustaffa; and Sulaiman, 2023).

On the other hand, studies in (Li et al., 2024 Li et al., 2024) proposed a hybrid PSO with Temporal Convolutional Network (TCN) for SoC estimation. The use of PSO helps the models learn the battery characteristics more effectively under varying conditions, while the TCN architecture is well-suited for handling the dynamic nature of battery data. Validated on public datasets, the findings suggest that the proposed method provides strong predictive performance. Meanwhile, a study in (Zhou et al., 2023) demonstrated an improved GWO to optimize the hyper parameters in Deep Extreme Learning Machine. A comparable investigation employing a hybrid PSO with Extreme Learning Machine for SoH estimation for LIBs is discussed in (Chen et al., 2024). Since its introduction back in 1995, the PSO has consistently demonstrated notable efficiency, leading to widespread and extensive use (Chen et al., 2024; Pan et al., 2023). Given the notable efficacy of PSO, this research introduces a hybrid approach that combines PSO with NN to predict the RUL of batteries. As emphasized earlier, the objective of this hybrid meta-heuristic optimization algorithm integrated with machine learning is to function as an optimizer for specific hyperparameters, namely, the network weights and hidden layer biases. The devised PSO—NN model was subsequently applied for the estimation of the RUL of batteries.

The major contributions of this study can be described as follows:

- Introduction of the PSO—NN hybrid model for accurate RUL estimation in batteries. Leveraging the proven efficiency of PSO as a metaheuristic optimization algorithm to enhance the performance of neural networks in predicting battery health.
- Comprehensive evaluation comparing the PSO—NN model with alternative algorithms, including Cultural Algorithm (CA-NN), Harmony Search Algorithm (HSA-NN), and Autoregressive Integrated Moving Average (ARIMA). Establishing the superior accuracy and efficiency of developed PSO—NN model in RUL predictions, contributing to proactive maintenance planning, resource optimization, and safety enhancement in diverse applications especially in electric vehicles (EVs).

The subsequent sections of the paper follow this structure: Section 2 delivers an insight into PSO, whereas Section 3 details information about NN. Section 4 outlines the methodology implemented, incorporating the hybrid PSO—NN model. Section 5 discusses the obtained results, and finally, Section 6 encapsulates the paper's conclusion.

2. Particle swarm optimization

Introduced by Kennedy and Eberhart back in 1995 (Kennedy and Eberhart, 1995), PSO is classified as Swarm Intelligence (SI) algorithm which simulates social behavior of birds and fish, where individuals in a group coordinate their movements to achieve a common goal. PSO is a widely employed approach for approximating solutions in optimization and search challenges. In PSO, the historical personal optimal position of particle i is referred to as $Pbest_i$, while the historical neighborhood optimal position of particle i is noted as $Nbest_i$. Particle i is guided by $Pbest_i$ and $Nbest_i$ to transition from less promising areas to more favorable locations. The position and velocity of particle i in the tth generation are represented as $x_i(t)$ and $v_i(t)$, respectively. The updates for $x_i(t)$ and $v_i(t)$ are determined by the following formulas (1), (2):

$$v_i(t+1) = wv_i(t) + C_1r_1(Pbest_i(t) - x_i(t)) + C_2r_2(Nbest_i(t) - x_{i(t))} \tag{1}$$

$$x_i(t+1) = x_i\ (t) +\ v_i(t+1) \tag{2}$$

In this context, w represents the inertia weight that governs the influence of the previous velocity on the current velocity. Additionally, C_1 and C_2 stand for the individual learning factor and the social learning factor, respectively. Meanwhile, r_1 and r_2 denote random values evenly distributed in the range [0,1].

3. Neural network

A neural network (NN) is a computational model inspired by the human brain's structure and functioning. It comprises interconnected nodes, or neurons, organized into layers namely an input layer, a hidden layer, and an output layer. Its structure aims to establish a mapping relationship between input variables and output variables (He et al., 2024). NNs are used for various tasks, such as pattern recognition (Chen et al., 2022; Singh et al., 2023; Xue et al., 2023), classification, and regression. The core idea is to learn complex relationships within data by adjusting the weights and biases associated with connections between neurons.

In the context of estimating battery RUL, NN can be employed to analyze historical data and predict how much longer a battery is expected to operate before reaching the end of its useful life. Input features might include information about charging cycles, discharge rates, temperature, and other relevant parameters. The success of a neural network in estimating RUL is closely tied to its ability to generalize well to new, unseen data. Generalization is enhanced by determining optimal weights and biases during the training phase. These parameters are adjusted iteratively using an optimization algorithm (e.g., gradient descent) to minimize the difference between predicted and actual RUL values on the training dataset. By finding the right balance in weights

Table 1
Sample of dataset.

CI	DT (s)	Dec_3.6–3.4 V (s)	MVD. (V)	MVC (V)	T_4.15 V (s)	TCC(s)	CT (s)	RUL
15,045	1093	794.31	190.33	3.78	3.74	965.98	1484.38	6795.44
15,046	1094	793.62	188.27	3.78	3.74	964.38	1484.38	6798.12
15,047	1095	789.75	186.50	3.78	3.74	962.25	1484.25	6761.06
15,048	1096	785	185.71	3.78	3.74	958.71	1448.31	6757.62
15,049	1097	783.94	184.37	3.78	3.74	947.98	1448.38	6676.62
15,050	1098	782.88	184.37	3.78	3.74	944.38	1448.38	6732.19
15,051	1099	782.69	184	3.78	3.74	940.71	1448.31	6696.56
15,052	1100	780.31	183.52	3.774	3.74	940.713	1448.31	6696.75
15,053	1101	779.75	183.52	3.775	3.74	936.375	1448.38	6695.62
15,054	1102	778.12	183	3.774	3.74	933.637	1448.44	6703.81

* CI= Cycle index, DT= Discharge time, Dec_3.6–3.4V= Decrement 3.6–3.4 V, MVD= Max. Voltage Discharge, MVC= Minimum voltage charge, T_4.15V= Time at 4.15 V, TCC= Time constant current, CT= Charging time, and RUL= Remaining Useful Life.

Table 2
Sample of normalized dataset.

CI	DT (s)	Dec_3.6–3.4 V (s)	MVD. (V)	MVC (V)	T_4.15 V (s)	TCC(s)	CT (s)	RUL
0.9638	0.0008	0.4946	0.5576	0.5269	0.0035	0.0017	0.0077	0.0168
0.9647	0.0008	0.4946	0.5561	0.5276	0.0035	0.0017	0.0077	0.0159
0.9656	0.0008	0.4946	0.5553	0.5269	0.0035	0.0017	0.0077	0.0150
0.9665	0.0008	0.4946	0.5553	0.5276	0.0034	0.0016	0.0077	0.0141
0.9673	0.0008	0.4946	0.5553	0.5284	0.0034	0.0016	0.0076	0.0132
0.9682	0.0008	0.4946	0.5553	0.5291	0.0034	0.0016	0.0076	0.0124
0.9691	0.0008	0.4946	0.5545	0.5291	0.0034	0.0016	0.0076	0.0115
0.9700	0.0008	0.4946	0.5538	0.5291	0.0034	0.0016	0.0076	0.0106
0.9709	0.0008	0.4946	0.5545	0.5291	0.0034	0.0016	0.0076	0.0097
0.9718	0.0008	0.4946	0.5538	0.5291	0.0033	0.0016	0.0076	0.0088

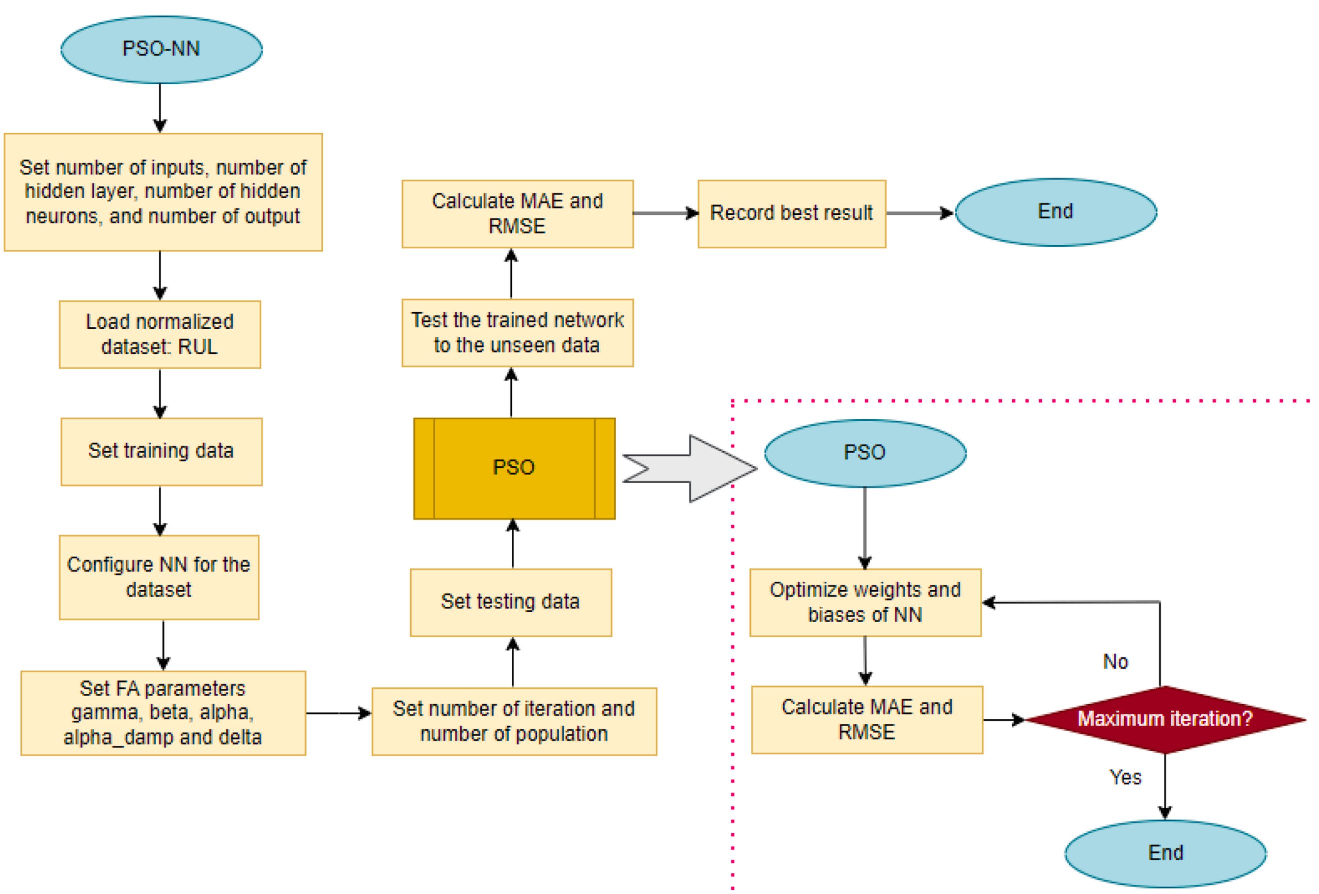

Fig. 1. Battery RUL Estimation based on hybrid PSO—NN.

and biases, the neural network becomes adept at capturing underlying patterns in the data, allowing it to make accurate predictions on new, unseen battery conditions.

Determining the optimal weights and biases is crucial to avoid overfitting (capturing noise in the training data) and underfitting (failing to capture essential patterns). Achieving a good balance helps the NN generalize well, making it effective in estimating battery RUL across various operating conditions.

4. Methodology

This section outlines the implemented methodology, covering diverse elements such as research data and data preparation, data preprocessing, experiment setup, the proposed PSO—NN for estimation of battery RUL, and examination of the evaluation and benchmark estimation model.

4.1. Research data and data preparation

In this study, a publicly available dataset was utilized, accessible from the Kaggle website (Aboelkhair et al., 2024). The dataset consists of 15,064 rows, encompassing 8 inputs: cycle number (CT), discharge time (s) (DT), decrement from 3.6 V to 3.4 V (s) (Dec_3.6–3.4 V), maximum voltage during discharge (V) (MVD), minimum voltage during charge (V) (MVC), time at 4.15 V (s) (T_4.15 V), time constant current (s) (TCC), and charging time (s) (CT). The sole output variable is the RUL. Table 1 shows the sample of dataset of input-output configurations in this study.

4.2. Data pre-processing

To enhance the learning process of the PSO—NN algorithm, the battery feature data undergo min–max normalization, scaling them to the range of (0, 1). The main objective was to avoid the dominance of larger input values over smaller ones, thereby potentially improving estimation accuracy. The Min-Max Normalization is expressed by the following equation:

$$v' = \left(\frac{v - min_a}{max_a - min_a}\right) * (newmax_a - newmin_a) + newmin_a \tag{3}$$

Where v' represents the new value for variable v, v is the current value, $min_a$is the minimum value in the data set; max_a is the maximum value in the dataset, newmax_a is the new maximum value in the dataset, and newmin_a is the new minimum value in the dataset. Min-Max normalization transforms a value of v of A to v' within the range $[newmax_a, newmin_a]$ by solving the above equation. The normalized dataset for the sample in Table 2 is presented in Table 2.

4.3. Training and testing

The dataset is divided into two distinct subsets: a training set, utilized for model fitting, and a testing set, employed for a genuine evaluation of the model's generalization performance. The split between these subsets follows a proportion of 0.7:0.3.

4.4. PSO—NN for estimation of battery RUL

This illustration depicts the operational flow of a hybrid PSO—NN model (see Fig. 1). In this framework, PSO is employed to optimize the weights and biases of the NN, which comprises 8 inputs, 1 hidden layer with 9 neurons, and 1 output. The iteration process continues until reaching a maximum of 1000 iterations. The dataset undergoes normalization and is subsequently partitioned into training and testing subsets before being input into the NN. This practice is crucial for preventing overfitting and enhancing generalization. The NN is tailored to the dataset by configuring essential hyperparameters such as the number of inputs, hidden layers, hidden neurons, and outputs. These parameters significantly impact the NN's performance.

Prior to optimizing the NN's weights and biases, PSO parameters including gamma, beta, alpha, alpha_damp, and delta are pre-set. These parameters govern the behavior and convergence rate of the PSO algorithm. Evaluation of the NN's performance involves calculating the Mean Absolute Error (MAE) and Root Mean Square Error (RMSE). These widely used error metrics quantify the disparity between actual and predicted values. The trained NN undergoes testing on unseen data to assess its accuracy and robustness. The optimization process concludes with the recording of the best result achieved.

4.5. Evaluation

Selecting a suitable performance evaluation metric is essential for validating the results obtained in the experiment. In this study, three statistical indices are employed: the Mean Absolute Error (MAE) and Root Mean Square Error (RMSE). RMSE assesses performance by giving greater importance to large estimation errors, while MAE treats all estimation errors equally without assigning varying weights. The formulas for MAE and RMSE are illustrated in the following equations:

$$MAE = \frac{1}{N}\sqrt{\sum_{i=1}^{N} |y(i) - \widehat{y}(i)|} \tag{4}$$

$$RMSE = \sqrt{\frac{\sum_{i=1}^{N} \| y(i) - \widehat{y}(i) \|^2}{N}} \tag{5}$$

Here, N represents the data length of the battery RUL under evaluation, with $y(i)$ and $\hat{y}(i)$ denoting the target and estimated battery RUL, respectively. Meanwhile, $\overline{O}$ is the mean of target values.

4.6. Benchmark estimation models

To facilitate comparison, the PSO—NN is assessed alongside other models, including the NN hybridized with Harmony Search Algorithm (Woo Geem et al., 2001) (HSA-NN), Cultural Algorithm (CA-NN), and Autoregressive Integrated Moving Average (ARIMA).

4.6.1. Harmony search algorithm

HSA is a heuristic optimization algorithm inspired by the improvisation process of musicians in a jazz ensemble (Woo Geem et al., 2001). The algorithm mimics the process by which musicians harmonize their notes to find an optimal solution to a problem. The algorithm begins with the initialization phase, where the initial population of potential solutions, called "harmonies", is initialized. Harmonies are selected from the population based on their fitness values, where the better-performing solutions are more likely to be included in the harmony memory. New harmonies are generated by adjusting the pitches (values) of existing harmonies. This process embodies the balance between exploration and exploitation in the search for improved solutions.

4.6.2. Cultural algorithm

Cultural Algorithms (CA) (Reynolds, 1994) fall under the domain of evolutionary computation, integrating a knowledge component referred to as the belief space along with the population component. In this context, Cultural Algorithms can be seen as an extension of the traditional genetic algorithm. Much like several other metaheuristic algorithms, CA starts with an initialization stage, involving the establishment of candidate solutions and the belief space, representing cultural knowledge. During the evaluation phase, the fitness or objective function of individuals within the population is appraised, and the belief space undergoes updates based on their performance and experiences. Similar to the Genetic Algorithm (GA) (Haupt and Haupt, 2004), CA

Table 3
Estimation of Battery RUL: PSO—NN vs. HSA-NN vs. CA-NN vs. ARIMA.

	MAE	RMSE	Maximum Error
PSO—NN	**2.7708**	**4.3468**	**104.7381**
HSA-NN	22.0583	34.5154	490.3125
CA-NN	9.1189	22.4646	827.0163
ARIMA	494.6275	584.3098	1.16×10^3

incorporates crossover and mutation operators to generate fresh candidate solutions. In the selection phase, individuals are chosen based on their fitness values or a combination of fitness and cultural knowledge.

4.6.3. ARIMA

ARIMA, which stands for Auto-Regressive Integrated Moving Average, is a popular time series forecasting method. It is a statistical model that combines autoregression, differencing, and moving average components to capture and predict patterns in time series data. ARIMA models are widely used in various fields, including economics, finance, and environmental science, to make predictions based on historical data. ARIMA models are defined by three parameters: p, d, and q, where p is the order of the autoregressive component, d is the degree of differencing, and q is the order of the moving average component. By adjusting these parameters, ARIMA models can be tailored to suit different time series patterns, making them a versatile tool for time series forecasting.

5. Results and discussion

The data presented in Table 3, generated with 9 hidden neurons, 1000 iterations, and 30 populations for PSO, HSA, and CA, reveals significant results regarding the performance of the models. The PSO—NN model consistently demonstrates the lowest errors across all three metrics: MAE of 2.7708, RMSE of 4.3468, and Maximum Error of 104.7381. This superior performance highlights PSO—NN's effectiveness in accurately predicting battery RUL. In contrast, both HSA-NN and CA-NN show moderate error levels. Specifically, CA-NN exhibits a higher MAE and RMSE compared to HSA-NN, indicating that while it is more accurate than ARIMA, it still falls short of PSO—NN. Notably, CA-NN's significantly higher Maximum Error suggests a vulnerability to outliers or noise within the dataset, leading to larger errors for certain instances.

ARIMA, on the other hand, presents considerably higher error rates, with an MAE of 494.6275, an RMSE of 584.3098, and a Maximum Error of 1.16×10^3. These results support observations in previous studies (He et al., 2024), which indicate that ARIMA struggles to handle nonlinearities in data due to its limited capacity to encapsulate complex dependencies between historical data points. Overall, these findings indicate that PSO—NN outperforms all other models in terms of accuracy and robustness. In contrast, ARIMA is the least effective, and CA-NN, while better than ARIMA, is less reliable compared to PSO—NN, particularly in handling outliers or noise

Fig. 2 depicts the alignment between the models (PSO—NN, HSA-NN, CA-NN, ARIMA) and the observed data in relation to battery RUL over time, which shows that the battery RUL decreases significantly over time, indicating that the battery degradation is a complex and dynamic process. A higher degree of proximity between the model and the observed data corresponds to superior prediction accuracy. From the visual representation, it is evident that PSO—NN outperforms the other models by closely adhering to the observed data. Conversely, CA-NN, HSA-NN, and ARIMA exhibit lower accuracy, as they display more frequent deviations from the observed data. Additionally, the figure illustrates substantial fluctuations in battery RUL over time, underscoring the intricate and dynamic nature of the battery degradation process.

The close-up views of estimated values are visualized in Figs. 3(a) and 3(b), offering a detailed comparison of different prediction models. These figures clearly demonstrate that the values generated by PSO—NN consistently align more closely with the observed patterns, indicating its superior performance in predicting Battery RUL. In contrast, CA-NN exhibits significant difficulties in consistently producing accurate values, often resulting in scattered outputs that consistently underestimate the true Battery RUL. This underestimation is particularly evident in both figures, where the CA-NN predictions consistently fall below the observed data points. Meanwhile, HSA-NN, while sometimes tracking the general trend, occasionally deviates dramatically from the observed values. These substantial deviations are especially pronounced in Fig. 3 (b), where HSA-NN shows sharp fluctuations at the beginning of the time

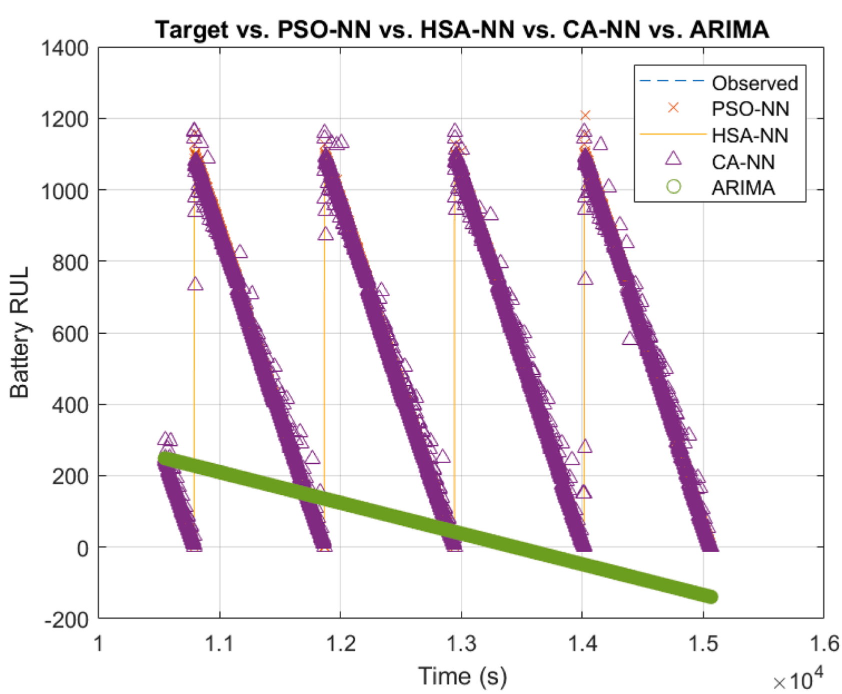

Fig. 2. Comparison of PSO—NN vs. Identified algorithms for battery RUL.

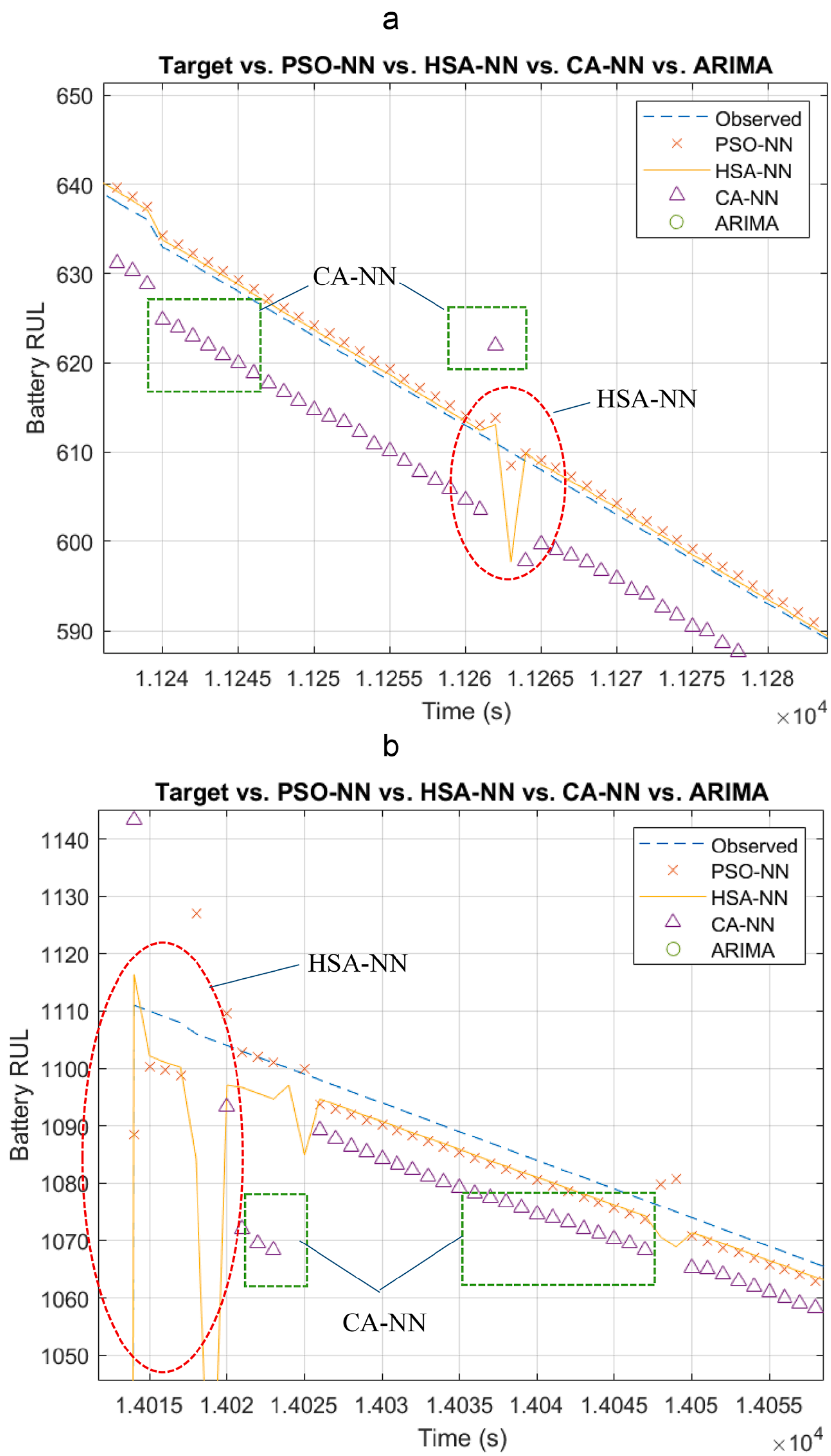

Fig. 3. (b): Zooming in - PSO—NN vs. Identified Algorithms for Battery RUL.

series. Such inconsistencies in the HSA-NN model's performance notably impact its recorded MAE, RMSE, and maximum error metrics, highlighting the challenges it faces in maintaining prediction accuracy across different time windows. The comparative analysis of these models underscores the robustness and reliability of the PSO—NN approach in accurately forecasting Battery RUL across varying conditions and time frames.

The illustration in Fig. 4 illustrates the convergence rates of three algorithms: PSO—NN, CA-NN, and HSA-NN. Each algorithm's performance is assessed utilizing the Mean Squared Error (MSE) metric. The x-axis denotes the number of iterations, ranging from 0 to 1000, while the y-axis represents the MSE values within the range of 0 to 0.04. Upon examination of the figure, it is evident that PSO—NN (depicted in blue with square markers) demonstrates swift convergence to the minimum MSE value. In contrast, CA-NN (depicted in orange with cross markers) converges at a marginally higher MSE value than PSO—NN. HSA-NN (depicted in red with dot markers) converges with the highest final MSE value.

Regarding algorithmic performance, PSO—NN achieves the most favorable outcome with the lowest MSE (approximately 0.0000609).

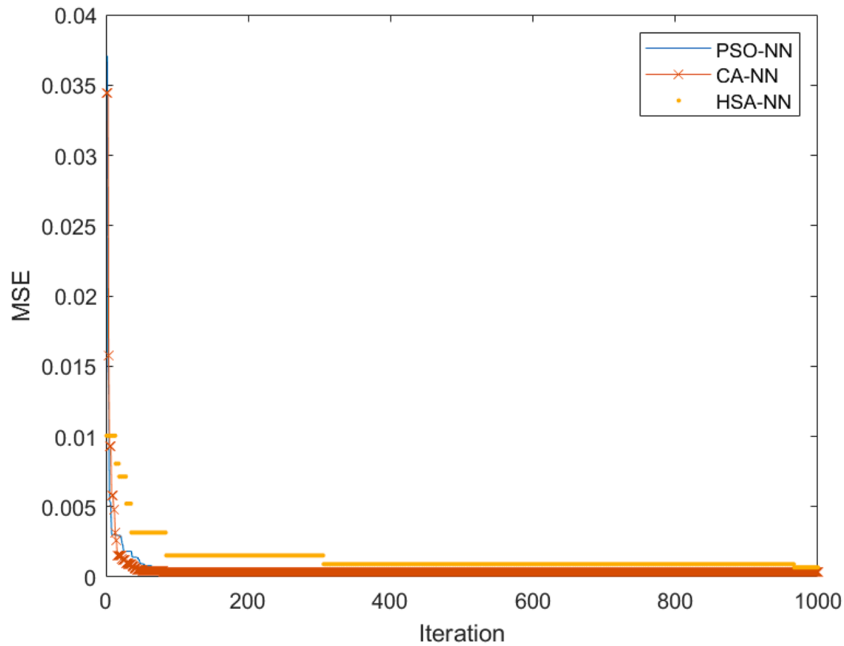

Fig. 4. Convergence rate: PSO—NN vs. Identified algorithms for battery RUL.

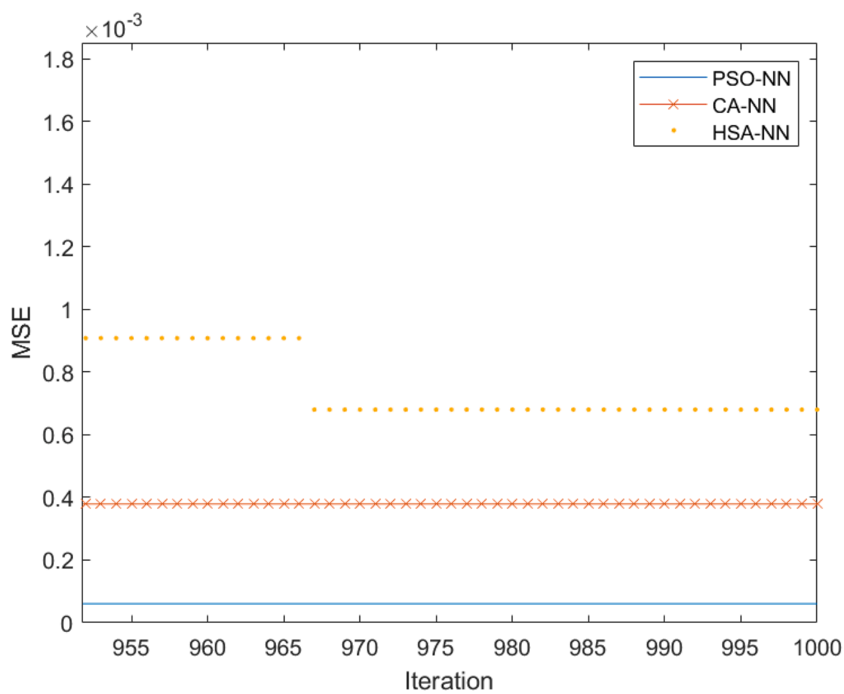

Fig. 5. Detailed examination of convergence rate: PSO—NN vs. Identified algorithms for battery RUL.

Table 4
Results of Two-Tail Probability (P($T \leq t$)) Between PSO—NN, HSA-NN, CA-NN, and PSO-ARIMA Models.

Methods	P($T \leq t$) two-tail
PSO—NN vs. HSA-NN	0.0012
PSO—NN vs. CA-NN	0.0000
PSO—NN vs. ARIMA	0.0000

CA-NN exhibits a higher MSE (approximately 0.0003787), while HSA-NN presents the highest MSE (approximately 0.0006799). The findings suggest that PSO—NN emerges as the most efficient algorithm in terms of convergence. CA-NN performs adequately but trails behind PSO—NN. HSA-NN displays the slowest convergence rate and the highest error.

The close-up of Fig. 4 is illustrated in Fig. 5. The figure clearly illustrates the differences in the recorded convergence rates for each method.

Table 4 shows the obtained result from Two-Tail Probability (P($T \leq t$) between the proposed PSO—NN and the three identified models. For PSO—NN vs. HSA-NN, the probability value of 0.0012 suggests a low likelihood of observing the observed difference (or more extreme) between PSO—NN and HSA-NN purely by chance. This indicates a statistically significant difference between the two methods. Meanwhile, for PSO—NN vs. CA-NN and PSO—NN vs. ARIMA, the probability value of 0.0000 indicates an extremely low likelihood of observing the observed difference (or more extreme) between PSO—NN and CA-NN, as well as PSO—NN and ARIMA, by chance.

In summary, the probability values in the table suggest statistically significant differences between PSO—NN and each of HSA-NN, CA-NN, and ARIMA. The smaller the probability value, the stronger the evidence against the null hypothesis of no difference between the compared methods.

The obtained results prove that our PSO—NN method excels in MAE, RMSE, and maximum error due to its effective optimization and learning capabilities. The PSO algorithm efficiently fine-tunes the neural network's parameters, enhancing accuracy by exploring and exploiting the solution space effectively. This combination allows the model to capture complex data patterns more effectively than other methods. Additionally, the two-tailed test confirms that these performance improvements are statistically significant.

Based on the findings of the study, the PSO—NN model for battery RUL estimation offers several quantifiable benefits in terms of cleaner and more sustainable energy systems. By providing accurate RUL predictions, the model enhances the efficiency of battery usage and maintenance, leading to reduced energy consumption. This improved efficiency translates into less wasteful energy use in battery-operated systems. Additionally, the model supports better battery management and recycling processes, thereby decreasing the frequency of battery replacements and minimizing environmental impact through reduced emissions and waste. By enabling timely maintenance and optimal resource use, the PSO—NN model promotes the adoption of more sustainable battery management practices. Overall, the integration of PSO with NN not only extends battery life but also supports cleaner energy technologies and contributes to more sustainable energy systems.

6. Conclusion

This study has successfully introduced the PSO—NN model for estimating battery RUL, demonstrating its effectiveness through a detailed evaluation. The PSO—NN model, which integrates Particle Swarm Optimization (PSO) with Neural Networks (NN), achieved superior performance in predicting battery RUL compared to alternative models. The results show that PSO—NN consistently produced the lowest Mean Absolute Error (MAE) of 2.7708 and Root Mean Squared Error (RMSE) of 4.3468, outperforming the CA-NN, HSA-NN, and ARIMA models. The statistical analysis confirms the significance of these differences, with Two-Tail Probability ($P(T \leq t)$) values all below the 0.05 significance level, indicating that PSO—NN's performance is statistically superior to that of the other methods. Additionally, PSO—NN exhibited the lowest maximum error and the fastest convergence rate, as evidenced by its performance metrics.

While the PSO—NN demonstrates strong performance in optimizing battery RUL estimation, there are several limitations that should be considered. First, the optimization process may become computationally intensive as the size of the dataset or the complexity of the NN increases. This could impact real-time applications, where both accuracy and speed are critical. Second, the PSO's convergence behavior, although faster in this study, might vary depending on the initialization parameters, potentially affecting the stability of results in different scenarios. Another limitation is that the model's performance has only been evaluated on the current dataset, which may limit the generalizability of the conclusions. The influence of external factors, such as environmental conditions or battery degradation modes not captured in the dataset, may also reduce the robustness of the model in real-world applications. Addressing these limitations in future work could provide a more comprehensive understanding of the proposed model's potential and limitations in diverse scenarios.

To address these limitations, future work could explore additional datasets to assess the generalizability of the PSO—NN model across diverse conditions. Investigating the optimization of hyperparameters could also enhance the model's adaptability to varying scenarios. Furthermore, exploring real-time implementation and improving computational efficiency would contribute to the practical application of the proposed approach in operational environments.

CRediT authorship contribution statement

Zuriani Mustaffa: Writing – original draft, Visualization, Methodology, Formal analysis, Data curation. **Mohd Herwan Sulaiman:** Writing – review & editing, Investigation, Conceptualization.

Declaration of competing interest

The authors declare that they have no known competing financial interests or personal relationships that could have appeared to influence the work reported in this paper.

Data availability

Data sharing not applicable to this article as datasets can be obtained from the literature.

Acknowledgement

This research is supported by Ministry of Higher Education Malaysia (MoHE) through research gran FRGS/1/2024/ICT02/UMP/02/2 and Universiti Malaysia Pahang Al-Sultan Abdullah, under research grant #RDU220379.

References

A.H. Aboelkhair, N. a. Hamed, O. Reda, N. Nabil, O. Ghanem, and O. Assal. "RUL analysis & machine learning." https://www.kaggle.com/code/ahmedhatem404/rul-analysis-machine-learnig/notebook (accessed 22 January 2024, 2024).

Abut, S., Okut, H., Kallail, K.J., 2024. Paradigm shift from artificial neural networks (ANNs) to deep convolutional neural networks (DCNNs) in the field of medical image processing. Expert. Syst. Appl. 244, 122983. https://doi.org/10.1016/j.eswa.2023.122983, 2024/06/15/.

Alsuwian, T., et al., 2024. A review of expert hybrid and co-estimation techniques for SOH and RUL estimation in battery management system with electric vehicle application. Expert. Syst. Appl. 246, 123123. https://doi.org/10.1016/j.eswa.2023.123123, 2024/07/15/.

Chen, K., et al., 2024. State of health estimation for lithium-ion battery based on particle swarm optimization algorithm and extreme learning machine. Green Energy Intellig. Transport., 100151 https://doi.org/10.1016/j.geits.2024.100151, 2024/01/07/.

Chen, S., Zhang, Y., Hou, X., Shang, Y., Yang, P., 2022. Wafer map failure pattern recognition based on deep convolutional neural network. Expert. Syst. Appl. 209, 118254. https://doi.org/10.1016/j.eswa.2022.118254, 2022/12/15/.

Dou, J., et al., 2022. Extreme learning machine model for state-of-charge estimation of lithium-ion battery using salp swarm algorithm. J. Energy Storage 52, 104996. https://doi.org/10.1016/j.est.2022.104996, 2022/08/25/.

Duan, W., Song, S., Xiao, F., Chen, Y., Peng, S., Song, C., 2023. Battery SOH estimation and RUL prediction framework based on variable forgetting factor online sequential extreme learning machine and particle filter. J. Energy Storage 65, 107322. https://doi.org/10.1016/j.est.2023.107322, 2023/08/15/.

Gonzalez, J., Yu, W., Telesca, L., 2022. Gated recurrent units based recurrent neural network for forecasting the characteristics of the next earthquake. Cybern. Syst. 53 (2), 209–222.

Gupta, R., Nalavade, J.E., 2023. Metaheuristic assisted hybrid classifier for bitcoin price prediction. Cybern. Syst. 54 (7), 1037–1061.

Haupt, R.L., Haupt, Sue Ellen, 2004. Practical genetic algorithms, 2nd edition. John Wiley & Sons, Inc., Publication, New Jersey.

Hayati, R., Munawar, A.A., Lukitaningsih, E., Earlia, N., Karma, T., Idroes, R., 2024. Combination of PCA with LDA and SVM classifiers: a model for determining the geographical origin of coconut in the coastal plantation, Aceh Province, Indonesia. Case Stud. Chem. Environm. Eng. 9, 100552. https://doi.org/10.1016/j.cscee.2023.100552, 2024/06/01/.

He, Z., Zhang, X., Fu, X., Pan, C., Jin, Y., 2024. Research on battery state of charge estimation based on variable window adaptive extended Kalman filter. Int. J. Electrochem. Sci. 19 (1), 100440. https://doi.org/10.1016/j.ijoes.2023.100440, 2024/01/01/.

Kennedy, J., Eberhart, R., 1995. Particle swarm optimization. In: Proceedings of ICNN'95 - International conference on neural networks, 4, pp. 1942–1948. https://doi.org/10.1109/ICNN.1995.488968, 27 Nov.1 Dec. 1995vol.4.

Korkmaz, M., 2023. SoC estimation of lithium-ion batteries based on machine learning techniques: a filtered approach. J. Energy Storage 72, 108268. https://doi.org/10.1016/j.est.2023.108268, 2023/11/15/.

Li, F., Zuo, W., Zhou, K., Li, Q., Huang, Y., 2024. State of charge estimation of lithium-ion batteries based on PSO-TCN-Attention neural network. J. Energy Storage 84, 110806. https://doi.org/10.1016/j.est.2024.110806, 2024/04/15/.

Li, F., Zuo, W., Zhou, K., Li, Q., Huang, Y., Zhang, G., 2024. State-of-charge estimation of lithium-ion battery based on second order resistor-capacitance circuit-PSO-TCN model. Energy 289, 130025. https://doi.org/10.1016/j.energy.2023.130025, 2024/02/15/.

Li, J., et al., 2022. Multi-objective optimization of mini U-channel cold plate with SiO2 nanofluid by RSM and NSGA-II. Energy 242, 123039. https://doi.org/10.1016/j.energy.2021.123039, 2022/03/01/.

Li, R., Li, W., Zhang, H., 2022. State of health and charge estimation based on adaptive boosting integrated with particle swarm optimization/support vector machine (AdaBoost-PSO-SVM) model for lithium-ion batteries. Int. J. Electrochem. Sci. 17 (2), 220212. https://doi.org/10.20964/2022.02.03, 2022/02/01/.

Li, Y., et al., 2022. A hybrid machine learning framework for joint SOC and SOH estimation of lithium-ion batteries assisted with fiber sensor measurements. Appl. Energy 325, 119787. https://doi.org/10.1016/j.apenergy.2022.119787, 2022/11/01/.

Li, Y., Ye, M., Wang, Q., Lian, G., Xia, B., 2024. An improved model combining machine learning and kalman filtering architecture for state of charge estimation of lithium-ion batteries. Green Energy Intelligent Transport., 100163 https://doi.org/10.1016/j.geits.2024.100163, 2024/01/10/.

Liu, B., Wang, H., Tseng, M.L., Li, Z., 2022. State of charge estimation for lithium-ion batteries based on improved barnacle mating optimizer and support vector machine. J. Energy Storage 55, 105830. https://doi.org/10.1016/j.est.2022.105830, 2022/11/30/.

Mall, P.K., et al., 2023. A comprehensive review of deep neural networks for medical image processing: recent developments and future opportunities. Healthcare Analyt. 4, 100216. https://doi.org/10.1016/j.health.2023.100216, 2023/12/01/.

Marzouk, M., Elhakeem, A., Adel, K., 2024. Artificial neural networks applications in construction and building engineering (1991–2021): science mapping and visualization. Appl. Soft. Comput. 152, 111174. https://doi.org/10.1016/j.asoc.2023.111174, 2024/02/01/.

Maya, M., Yu, W., Telesca, L., 2022. Multi-step forecasting of earthquake magnitude using meta-learning based neural networks. Cybern. Syst. 53 (6), 563–580.

Mehta, C., Sant, A.V., Sharma, P., 2024. Optimized ANN for LiFePO4 battery charge estimation using principal components based feature generation. Green Energy Intell. Transport., 100175 https://doi.org/10.1016/j.geits.2024.100175, 2024/01/17/.

Mendoza-Bernal, J., González-Vidal, A., Skarmeta, A.F., 2024. A convolutional neural network approach for image-based anomaly detection in smart agriculture. Expert. Syst. Appl. 247, 123210. https://doi.org/10.1016/j.eswa.2024.123210, 2024/08/01/.

Mirjalili, S., 2015. Moth-flame optimization algorithm: a novel nature-inspired heuristic paradigm. Knowl. Based. Syst. 89, 228–249. https://doi.org/10.1016/j.knosys.2015.07.006, 2015/11/01/.

Mirjalili, S., Gandomi, A.H., Mirjalili, S.Z., Saremi, S., Faris, H., Mirjalili, S.M., 2017. Salp Swarm Algorithm: a bio-inspired optimizer for engineering design problems. Adv. Eng. Software 114, 163–191. https://doi.org/10.1016/j.advengsoft.2017.07.002, 2017/12/01/.

Mirjalili, S., Mirjalili, S.M., Lewis, A., 2014. Grey Wolf Optimizer. Adv. Eng. Software 69, 46–61. https://doi.org/10.1016/j.advengsoft.2013.12.007, 2014/03/01/.

Mustaffa, Z., Sulaiman, M.H., 2023. Enhancing battery state of charge estimation through hybrid integration of barnacles mating optimizer with deep learning. Franklin Open 5, 100053. https://doi.org/10.1016/j.fraope.2023.100053, 2023/12/01/.

Pan, C., Li, Y., Wang, J., Liang, J., Jinyama, H., 2023. Research on multi-lane energy-saving driving strategy of connected electric vehicle based on vehicle speed prediction. Green Energy Intellig. Transport. 2 (6), 100127. https://doi.org/10.1016/j.geits.2023.100127, 2023/12/01/.

Rauf, H., Khalid, M., Arshad, N., 2022. Machine learning in state of health and remaining useful life estimation: theoretical and technological development in battery degradation modelling. Renew. Sustain. Energy Rev. 156, 111903. https://doi.org/10.1016/j.rser.2021.111903, 2022/03/01/.

Reynolds, R.G., 1994. An Introduction to Cultural Algorithm. In: Proceedings of the 3rd annual conference on evolutionary programming. World Scientific, San Diego, California, USA.

Singh, P., Prakash, A., Parida, S.K., 2023. Neural network based pattern recognition for classification of the forced and natural oscillation. Electric Power Syst. Res. 224, 109706. https://doi.org/10.1016/j.epsr.2023.109706, 2023/11/01/.

Sulaiman, M.H., Mustaffa, Z., 2024. State of charge estimation for electric vehicles using random forest. Green Energy Intellig. Transport., 100177 https://doi.org/10.1016/j.geits.2024.100177, 2024/01/19/.

Sulaiman, M.H., Mustaffa, Z., Saari, M.M., Daniyal, H., 2020. Barnacles mating optimizer: a new bio-inspired algorithm for solving engineering optimization problems. Eng. Appl. Artif. Intell. 87, 103330. https://doi.org/10.1016/j.engappai.2019.103330, 2020/01/01/.

Suykens, J.A.K., Gestel, T.V., Brabanter, Bart De Moor, De, Jos, Vandewalle, Joos, 2002. *Least squares support vector machines*. K U Leuven. World Scientific, Belgium, p. 308.

Tao, T., et al., 2024. Data-based health indicator extraction for battery SOH estimation via deep learning. J. Energy Storage 78, 109982. https://doi.org/10.1016/j.est.2023.109982, 2024/02/01/.

Vapnik, V.N., 1995. The nature of statistical learning theory, 2nd ed. Springer-Verlag, New York.

Vivian, J., Prataviera, E., Gastaldello, N., Zarrella, A., 2024. A comparison between grey-box models and neural networks for indoor air temperature prediction in buildings. J. Build. Eng. 84, 108583. https://doi.org/10.1016/j.jobe.2024.108583, 2024/05/01/.

Woo Geem, Zong, Kim, Joong Hoon, Loganathan, G.V., 2001. A new heuristic optimization algorithm: harmony search. Simulation. 76 (2), 60–68.

Xue, L., Wu, H., Zheng, H., He, Z., 2023. Control chart pattern recognition for imbalanced data based on multi-feature fusion using convolutional neural network. Comput. Ind. Eng. 182, 109410. https://doi.org/10.1016/j.cie.2023.109410, 2023/08/01/.

Zhang, S., Yang, L., Zhao, X., Qiang, J., 2015. A GA optimization for lithium–ion battery equalization based on SOC estimation by NN and FLC. Internat. J. Electr. Power Energy Syst. 73, 318–328. https://doi.org/10.1016/j.ijepes.2015.05.018, 2015/12/01/.

Zhang, Y., et al., 2022. Performance comparison between straight channel cold plate and inclined channel cold plate for thermal management of a prismatic LiFePO4 battery. Energy 248, 123637. https://doi.org/10.1016/j.energy.2022.123637, 2022/06/01/.

Zhou, Y., Wang, S., Xie, Y., Shen, X., Fernandez, C., 2023. Remaining useful life prediction and state of health diagnosis for lithium-ion batteries based on improved grey wolf optimization algorithm-deep extreme learning machine algorithm. Energy 285, 128761. https://doi.org/10.1016/j.energy.2023.128761, 2023/12/15/.

Zuo, W., et al., 2022. Effects of multi-factors on performance of an improved multi-channel cold plate for thermal management of a prismatic LiFePO4 battery. Energy 261, 125384. https://doi.org/10.1016/j.energy.2022.125384, 2022/12/15/.

Zuo, W., Li, D., Li, Q., Cheng, Q., Huang, Y., 2024. Effects of intermittent pulsating flow on the performance of multi-channel cold plate in electric vehicle lithium-ion battery pack. Energy 294, 130832. https://doi.org/10.1016/j.energy.2024.130832, 2024/05/01/.

Zuo, W., Zhang, Y., E, J., Li, J., Li, Q., Zhang, G., 2022. Performance comparison between single S-channel and double S-channel cold plate for thermal management of a prismatic LiFePO4 battery. Renew. Energy 192, 46–57. https://doi.org/10.1016/j.renene.2022.04.116, 2022/06/01/.